HHS Public Access

Author manuscript

AJR Am J Roentgenol. Author manuscript; available in PMC 2022 February 22.

Published in final edited form as:

AJR Am J Roentgenol. 2021 June ; 216(6): 1614–1625. doi:10.2214/AJR.20.24172.

Diagnostic Accuracy of Quantitative Multicontrast 5-Minute Knee MRI Using Prospective Artificial Intelligence Image Quality Enhancement

Akshay S. Chaudhari, PhD[1], **Murray J. Grissom, MD**[2], **Zhongnan Fang, PhD**[3], **Bragi Sveinsson, PhD**[4,5], **Jin Hyung Lee, PhD**[6,7,8,9], **Garry E. Gold, MD**[1,7,10], **Brian A. Hargreaves, PhD**[1,7,9], **Kathryn J. Stevens, MD**[1,10]

[1]Department of Radiology, Lucas Center for Imaging, Stanford University, 1201 Welch Rd, PS 055B, Stanford, CA 94305.

[2]Santa Clara Valley Medical Center, San Jose, CA.

[3]LVIS Corporation, Palo Alto, CA.

[4]Athinoula A. Martinos Center for Biomedical Imaging, Massachusetts General Hospital, Charlestown, MA.

[5]Department of Radiology, Harvard Medical School, Boston, MA.

[6]Department of Neurology and Neurological Sciences, Stanford University, Stanford, CA.

[7]Department of Bioengineering, Stanford University, Stanford, CA.

[8]Department of Neurosurgery, Stanford University, Stanford, CA.

[9]Department of Electrical Engineering, Stanford University, Stanford, CA.

[10]Department of Orthopaedic Surgery, Stanford University, Redwood City, CA.

Abstract

BACKGROUND.—Potential approaches for abbreviated knee MRI, including prospective acceleration with deep learning, have achieved limited clinical implementation.

OBJECTIVE.—The objective of this study was to evaluate the interreader agreement between conventional knee MRI and a 5-minute 3D quantitative double-echo steady-state (qDESS) sequence with automatic T2 mapping and deep learning super-resolutionaugmentation and to compare the diagnostic performance of the two methods regarding findings from arthroscopic surgery.

Address correspondence to A. S. Chaudhari (akshaysc@stanford.edu).

A. S. Chaudhari has provided consulting services to SkopeMR, Inc., Subtle Medical, Chondrometrics GmbH, Image Analysis Group, Edge Analytics, ICM, and Culvert Engineering and is a shareholder of Subtle Medical, LVIS Corporation, and Brain Key. J. H. Lee is the founder of LVIS Corporation. B. A. Hargreaves is a shareholder of LVIS Corporation. The remaining authors declare that they have no disclosures relevant to the subject matter of this article.

Based on a presentation at the International Skeletal Society 2019 annual meeting, Vancouver, BC, Canada.

An electronic supplement is available online at doi.org/10.2214/AJR.20.24172.

METHODS.—Fifty-one patients with knee pain underwent knee MRI that included an additional 3D qDESS sequence with automatic T2 mapping. Fourier interpolation was followed by prospective deep learning super resolution to enhance qDESS slice resolution twofold. A musculoskeletal radiologist and a radiology resident performed independent retrospective evaluations of articular cartilage, menisci, ligaments, bones, extensor mechanism, and synovium using conventional MRI. Following a 2-month washout period, readers reviewed qDESS images alone followed by qDESS with the automatic T2 maps. Interreader agreement between conventional MRI and qDESS was computed using percentage agreement and Cohen kappa. The sensitivity and specificity of conventional MRI, qDESS alone, and qDESS plus T2 mapping were compared with arthroscopic findings using exact McNemar tests.

RESULTS.—Conventional MRI and qDESS showed 92% agreement in evaluating all tissues. Kappa was 0.79 (95% CI, 0.76–0.81) across all imaging findings. In 43 patients who underwent arthroscopy, sensitivity and specificity were not significantly different ($p = .23$ to $> .99$) between conventional MRI (sensitivity, 58–93%; specificity, 27–87%) and qDESS alone (sensitivity, 54–90%; specificity, 23–91%) for cartilage, menisci, ligaments, and synovium. For grade 1 cartilage lesions, sensitivity and specificity were 33% and 56%, respectively, for conventional MRI; 23% and 53% for qDESS ($p = .81$); and 46% and 39% for qDESS with T2 mapping ($p = .80$). For grade 2A lesions, values were 27% and 53% for conventional MRI, 26% and 52% for qDESS ($p = .02$), and 58% and 40% for qDESS with T2 mapping ($p < .001$).

CONCLUSION.—The qDESS method prospectively augmented with deep learning showed strong interreader agreement with conventional knee MRI and near-equivalent diagnostic performance regarding arthroscopy. The ability of qDESS to automatically generate T2 maps increases sensitivity for cartilage abnormalities.

CLINICAL IMPACT.—Using prospective artificial intelligence to enhance qDESS image quality may facilitate an abbreviated knee MRI protocol while generating quantitative T2 maps.

Keywords

artificial intelligence; biomarkers; knee injuries; MRI; radiology

---

Conventional diagnostic MRI of the knee usually consists of 2D fast spin-echo (FSE) scans that offer excellent contrast and in-plane resolution at the cost of thick slices and slice gaps. Therefore, scanning with the same image contrasts in orthogonal scan planes is necessary, and multiplanar and oblique reformations are not possible. Recent interest in abbreviated and high-value knee MRI protocols has led to advances in 3D FSE sequences for improving diagnostic efficiency [1–3]. Three-dimensional FSE sequences have shown promising diagnostic utility; however, compared with 2D FSE scans, 3D FSE images show increased blurring due to the long echo trains, which has limited widespread clinical implementation [4, 5]. Similarly, multicontrast sequences such as T2 shuffling have also shown diagnostic utility, but broad implementation remains challenging because of long reconstruction durations [6].

The 3D quantitative double-echo steady-state (qDESS) method may be promising for efficient diagnostic knee MRI [7, 8]. The technique produces two echoes: the first echo (S+) has T2/T1 weighting, and the second echo (S–) has higher T2 weighting. This differs

from the DESS sequence traditionally implemented as a Siemens Healthineers product, which combines the two qDESS echoes into a single composite image. Separating the two echoes can provide independent image contrasts and accurate T2 parameter maps [8–10]. The T2 relaxation time of cartilage is commonly measured in knee osteoarthritis imaging studies but currently has a limited role in diagnostic imaging [11, 12]. Despite evidence suggesting that changes in cartilage T2 relaxation times precede morphologic changes, the long scan durations required for acquiring T2 maps have inhibited clinical implementation in a diagnostic setting [13]. A prior study showed the potential diagnostic prowess of qDESS; however, the sequence was limited by through-plane blurring, and the T2 maps were not evaluated as part of the diagnostic examination [14].

MRI acceleration methods such as compressed sensing, parallel imaging, and simultaneous multislice acquisitions can expedite image acquisition but can result in hand-crafted regularization parameters, higher g-factors, or lower signal-to-noise ratios due to reduced TR [15, 16]. Deep learning–based techniques have successfully been explored in different imaging modalities [17–19]. In particular, super resolution has the ability to retrospectively enhance the resolution of acquired MRI data [20]. In knee MRI, super resolution has been shown to outperform conventional slice-direction Fourier interpolation, which is commonly performed directly on MRI scanners, while maintaining sensitivity to subtle changes in articular cartilage morphology and early osteophytes [21, 22]. Enhancing the slice resolution in knee MRI compared with Fourier interpolation without increasing scan time may allow the acquisition of a single rapid sequence that can be reformatted into arbitrary scan planes while maintaining adequate diagnostic accuracy.

In this study, we evaluated a 5-minute 3D qDESS sequence that automatically generates T2 relaxation time maps and is augmented with deep learning–based super resolution to enhance Fourier interpolation image quality. We assessed interreader agreement of conventional knee MRI and the qDESS sequence and compared the diagnostic performance of the two methods with respect to findings from arthroscopic surgery.

Materials and Methods

Patient Recruitment

This study was HIPAA compliant and received institutional review board approval with written informed consent from all participants. A total of 301 consecutive patients with knee pain underwent routine knee MRI at our institution between July 2016 and November 2017. MRI examinations included an additional qDESS sequence. The scans from 49 patients were used to fine-tune the deep learning–based super-resolution enhancement, leaving 252 patients who were potentially eligible for inclusion. Of these 252 patients, 51 underwent subsequent surgery and were included in the final study sample for retrospective image analysis using qDESS and deep learning–based super-resolution image quality enhancement. No patients were excluded after their MRI examination.

MRI Protocol

All MRI scans were performed on one of two identical 3-T MRI scanners (Discovery MR750, GE Healthcare) using an 8-channel transmit-receive knee coil. A 5-minute sagittal 3D qDESS sequence with a spatial-spectral pulse for water excitation was added to the standard diagnostic knee MRI protocol and consisted of five 2D FSE sequences. Table 1 shows scan parameters, and Figure S1 (in the *AJR* electronic supplement to this article, available at doi.org/10.2214/AJR.20.24172) presents example images. Reconstructed qDESS images and T2 relaxation maps were created automatically on the scanner computer and submitted immediately to the PACS as separate DICOM series [8, 10]. The duration of the conventional imaging protocol, excluding the localizer scan, was measured using DICOM headers.

Super-Resolution Enhancement

Of the 301 qDESS scans, 252 were acquired with 1.6-mm slice resolution and interpolated to 0.8 mm with the imager's ZIP2 feature; the remaining 49 were acquired with true 0.8-mm slice resolution. The goal of the deep learning–based super-resolution image enhancement was to outperform the ZIP2 Fourier interpolation software provided directly on the scanner and to improve the slice resolution from 1.6 to 0.8 mm. A convolutional neural network was initially developed to enhance slice resolution twofold from 1.4 to 0.7 mm using 176 3D DESS scans from the Osteoarthritis Initiative [21]. Subsequently, this network was fine-tuned using transfer learning on the 49 qDESS scans with higher slice resolution.

Overall, the deep learning–based super-resolution algorithm was trained to decrease qDESS scan slice thickness from 1.6 to 0.8 mm. The 51 patients who underwent arthroscopic surgery and were included in the study sample were not included in the super-resolution network training and thus represented a true independent test set. Figure 1 provides a flowchart of the overall convolutional neural network and patient inclusion.

Image Interpretation

A fellowship-trained musculoskeletal radiologist (K.J.S.) with 20 years of experience and a second-year radiology resident (M.J.G.) independently reviewed all MRI studies using the Horos DICOM viewer (Horos Project), which can reformat the sagittal qDESS images into coronal, axial, or oblique planes. The readers were not given the original imaging interpretations or surgical reports. The readers first reviewed images from conventional MRI and then, after a 2-month washout period, reviewed qDESS images separately. The readers scored the diagnostic quality of each protocol using a 5-point scale (1, very poor; 2, poor; 3, acceptable; 4, good; 5, very good).

The following structures were evaluated for the presence or absence of imaging abnormalities: ligaments (anterior and posterior cruciate ligaments, medial and lateral collateral ligaments) were assessed for low-grade sprain, moderate-grade sprain, or complete tear; menisci were assessed for myxoid degeneration or horizontal, radial, vertical longitudinal, complex, and complex flap tears in the anterior horn, body, or posterior horn of the medial and lateral menisci; cartilage lesions were graded as 0 (normal), 1 (increased T2 signal in morphologically normal-appearing cartilage), 2A (≤ 50% thickness

chondral defect), 2B (> 50% thickness chondral defect), or 3 (full thickness chondral defect) according to the modified Noyes criteria [23]; bone was evaluated for the presence or absence of bone marrow edema–like signal, subchondral cyst, or fracture; the extensor mechanism was assessed for tendinopathy and partial or complete tears of quadriceps or patellar tendons (or both); and the synovium was evaluated for synovitis and the presence of joint effusion graded as small, moderate, or large (on an ordinal scale of 0–3). Cartilage lesions and osseous abnormalities were evaluated in the medial and lateral femoral condyles, medial and lateral tibial plateaus, femoral trochlea, and patella [24]. Multiple osseous abnormalities could be evaluated in the same anatomic subregion. Consequently, each patient could have up to six and 18 cartilage and osseous findings, respectively.

During the qDESS image review, the readers first reviewed the two morphologic images and generated a report of their findings. After the qDESS morphologic image review, the readers reviewed the T2 relaxation time maps and provided new findings, if any (qDESS plus T2 findings). The readers were asked to indicate whether inclusion of the T2 map increased their diagnostic confidence. After the qDESS plus T2 readings, the readers viewed the coronal proton density (PD)–weighted fat-saturated (FS) sequence and provided new findings, if any, based on previous descriptions of interpretations of these sequences [14]. For the additional reviews using the T2 maps and the PD-weighted FS sequence, the readers were allowed to modify their original interpretations for all assessed tissues (cartilage, cruciate and collateral ligaments, meniscus, extensor mechanism, bone marrow, and synovium). A post hoc analysis was performed in cases with discrepant interpretations between conventional MRI and qDESS to identify the abnormalities present in such cases.

Arthroscopic Surgery

Surgery was performed by orthopedic surgeons who had access to the original MRI interpretations during surgery. All articular surfaces were evaluated during surgery according to the Noyes scale [23]. In the case of multiple lesions along the same articular surface, the largest lesion was scored. The presence of a partial or full-thickness tear of the anterior or posterior cruciate ligament, presence of medial or lateral meniscal tears (horizontal, radial, vertical longitudinal, complex, or complex flap tears), and the presence or absence of synovitis were documented during surgery [25]. Arthroscopic surgery results were only included for patients who underwent surgery within 3 months of their MRI examination. Of the 51 patients initially selected for imaging, six underwent surgery in the knee contralateral to the imaged knee, and two patients underwent surgery for posterior capsule repair and open quadriceps tendon repair, respectively, without a complete evaluation of the intraarticular structures. Consequently, full surgical reports were available for 43 patients.

Statistical Analysis

Data analysis was conducted according to previous studies that separately evaluated the diagnostic capabilities of a 3D FSE sequence for comprehensive knee MRI and the value of adding a T2 mapping sequence to the routine knee MRI protocol [4, 26]. The agreement between conventional MRI and qDESS for positive and negative findings, using conventional MRI as the comparison standard, was computed along with the 95% CI. Positive, negative, and total agreement between conventional MRI and qDESS were

computed for the full sample of 51 patients in lieu of sensitivity, specificity, and accuracy, respectively, given the absence of a reference standard on the basis of imaging alone. Positive agreement was defined as both conventional MRI and qDESS showing an abnormal finding, whereas negative agreement was defined as a given abnormality being absent on both. The added agreement from the inclusion of the T2 maps and the PD-weighted FS sequence was also evaluated.

The sensitivity, specificity, and accuracy of the conventional knee MRI sequences and the qDESS scans (with and without T2 maps) were computed with respect to the arthroscopic findings as the reference standard. Differences between the sensitivity and specificity confusion matrices for conventional MRI and qDESS were tested using exact McNemar tests. Wilcoxon signed rank tests were used to compare differences between the diagnostic image quality ratings provided for conventional MRI and qDESS. All comparisons between conventional MRI and qDESS were performed on the full group of 51 patients, whereas comparisons with arthroscopic surgery were performed on a sub-group of 43 patients. Significance levels for all statistical comparisons were set to $p < .05$.

Cohen linearly weighted kappa was used to evaluate interob-server agreement [27]. A Pearson correlation coefficient (r) was used to calculate the concordance between conventional MRI and qDESS regarding the size of joint effusion. To assess agreement between imaging methods, the qDESS findings for each reader were compared with the reader's own findings on conventional MRI. To assess diagnostic performance, conventional MRI findings and qDESS findings were separately compared with the arthroscopic findings, which served as the reference standard. Reported imaging abnormalities were grouped by tissue (articular cartilage, menisci, ligaments, bones, extensor mechanism, and synovium). All statistical analyses were performed by pooling imaging findings from both readers [4] and using the NumPy (version 1.12.1) and SciPy (version 0.19.1) libraries in Python (version 3.6.1, Python Software Foundation).

Results

The study sample included 34 men (mean age, 40 ± 16 [SD] years; range, 18–74 years) and 17 women (mean age, 52 ± 18 years; range, 25–98 years) who underwent knee MRI including the 5-minute 3D qDESS sequence with deep learning–based super-resolution image quality enhancement. The nominal combined scan time for the five conventional 2D FSE sequences was 15 minutes. However, the additional time required for prescanning and for scan prescriptions by technologists increased the mean total duration of the conventional 2D FSE protocol to 21 ± 2 minutes per patient, excluding localizer scans. The image quality enhancement with deep learning–based super-resolution compared with the native ZIP2 Fourier interpolation is shown in Figure S2 (available at doi.org/10.2214/AJR.20.24172), which presents coronal and axial multiplanar reformations of sagittal qDESS images depicting a complete tear of the superficial and deep fibers of the proximal medial collateral ligament.

Table 2 summarizes findings from conventional MRI, qDESS, and surgery. Table 3 presents the interreader agreement between conventional MRI and qDESS, including percentage

agreement and kappa values. Overall, the two imaging methods showed 92% agreement in findings from all tissues. The overall Cohen kappa value (0.79) showed substantial agreement for all imaging findings combined (95% CI, 0.76–0.81). Findings for the cruciate ligaments had the highest and almost perfect agreement between the two readers, with a kappa value of 0.85 (95% CI, 0.76–0.94). Findings for the extensor mechanism had the lowest agreement, although the kappa value was still substantial at 0.64 (95% CI, 0.52–0.76).

Table S1 (available at doi.org/10.2214/AJR.20.24172), compares the diagnostic image quality scores between conventional MRI and qDESS. The image quality scores were significantly better for conventional MRI for all evaluated tissues ($p < .001$). Nonetheless, qDESS showed acceptable diagnostic image quality for all tissues other than the collateral ligaments (mean image quality score, 2.7 ± 0.5). The size of joint effusions was highly correlated ($r = 0.90$) between conventional MRI and qDESS.

Conventional MRI and qDESS showed comparable sensitivity and specificity with respect to arthroscopic findings of injuries to the menisci (sensitivity, 93% vs 90%; specificity, 79% vs 80%; $p > .99$) and cruciate ligaments (sensitivity, 91% vs 86%; specificity, 87% vs 91%; $p = .23$). The overall accuracy across tissues was 65% for conventional MRI, 60% for qDESS, and 64% for qDESS plus T2. The qDESS plus T2 method had a higher sensitivity for detecting cartilage lesions (73%) compared with conventional MRI (58%) (Table 4). The T2 map increased the accuracy of qDESS detection of cartilage lesions from 60% to 64%. The T2 map also resulted in a modified diagnosis or increased diagnostic confidence in 41 of 51 patients and in 38% of all cartilage surfaces evaluated. Evaluation of the T2 map in combination with the qDESS images resulted in higher sensitivity, albeit lower specificity, for grade 1 and 2A cartilage lesions compared with conventional MRI (Table 5). The sensitivity and specificity for grade 1 cartilage lesions were 33% and 56% for conventional MRI, 23% and 53% for qDESS ($p = .81$), and 46% and 39% for qDESS plus T2 ($p = .80$). The sensitivity and specificity for grade 2A cartilage lesions were 27% and 53% for conventional MRI, 26% and 52% for qDESS ($p = .02$), and 58% and 40% for qDESS plus T2 ($p < .001$). Sensitivity for detecting bone marrow abnormalities was 68% (95% CI, 59–75%) for qDESS plus PD-weighted FS compared with 45% (95% CI, 37–54%) for qDESS alone. In one patient, the inclusion of a coronal PD-weighted FS sequence showed a complete tear of the medial collateral ligament that was not seen on qDESS.

A post hoc analysis of the discordant findings between qDESS and conventional MRI showed that low-to moderate-grade sprains accounted for 92% (12/13) of discordant qDESS findings in the anterior and posterior cruciate ligaments and 94% (17/18) of discordant findings in medial and lateral collateral ligaments. Similarly, myxoid degeneration accounted for 50% (11/22) of discordant qDESS findings in the menisci.

Figures 2 and 3 show example images from conventional MRI and qDESS for patients with arthroscopically confirmed oblique and bucket-handle meniscal tears, respectively. Both examples depict regions of articular cartilage that appear normal on the morphologic images but show focal changes on the qDESS T2 maps (see also Fig. S3). Similarly, Figure S4 (supplemental images available at doi.org/10.2214/AJR.20.24172), shows a vertical

meniscal peripheral tear and corresponding increase in cartilage T2 values in a patient with a complete anterior cruciate ligament tear. A high-grade tear of the posterior cruciate ligament accompanied by cartilage signal heterogeneity and hyperintense signal in the femoral trochlea is seen in Figure 4; qDESS images show the hypointense patellar cartilage signal well given the reduced partial volume artifacts compared with the T2-weighted MRI sequence. An example of a hypoplastic trochlea with similar conspicuity on conventional MRI and qDESS is shown in Figure S5.

Discussion

In this study, we showed the diagnostic utility of a 5-minute 3D qDESS MRI sequence that generates multicontrast images and simultaneous quantitative T2 relaxation time measurements and used deep learning to enhance Fourier interpolation image quality. This rapid sequence showed high concordance with imaging findings from an approximately 20-minute conventional diagnostic knee MRI protocol and had a sensitivity and specificity comparable with the conventional protocol when arthroscopic findings were used as the reference standard. Compared with previous studies evaluating qDESS without the use of deep learning–based super-resolution or T2 mapping, our study found considerably improved concordance between qDESS and arthroscopic results [14]. This rapid and comprehensive qDESS diagnostic scan minimizes the time patients spend in the scanner, which can benefit patients who are claustrophobic or experiencing pain and potentially increase clinical throughput. The automatic T2 relaxation time maps depicted early chondral degeneration, with respect to arthroscopic findings, within areas that appeared as morphologically normal articular cartilage on conventional sequences. The addition of a 2-minute PD-weighted FS sequence increased sensitivity to osseous findings, which may provide a practical path for a targeted quantitative knee MRI protocol.

The novelty of this work compared with previous studies of rapid imaging protocols is the simultaneous acquisition of anatomic and quantitative imaging along with the incorporation of quantitative T2 mapping into the MRI interpretation. Additionally, our study presents a prospective implementation of deep learning to enhance image quality from lower-resolution acquired data as opposed to a simply retrospective undersampling of high-resolution data, as is more commonly performed [28]. To our knowledge, this is the first study to use both simultaneous T2 map generation and analysis for evaluating knee internal derangement and prospective deep learning for 3D knee MRI. Depending on institutional needs, qDESS may first be included as an add-on scan to generate T2 relaxation time maps while radiologists become familiar with the contrast in the images. Subsequently, qDESS has the potential to replace one or more sequences from the routine imaging sequences, such as the sagittal PD-weighted or sagittal T2-weighted FS sequence.

Observations on the qDESS images correlated well with findings from conventional MRI in the detection of meniscus, cartilage, ligament, and synovium abnormalities. In the past, gradient-echo-based sequences such as DESS (where the two qDESS echoes are combined) have underestimated focal articular cartilage defects. However, with the separated echoes, the higher T2 weighting of the second qDESS echo is generated from refocusing pathways that lengthen the effective TE. Because this qDESS echo has a lower signal than the mixed

T2- and T1-weighted echo, the contrast of the combined echoes is dominated by the latter, leading to lower sensitivity in the detection of chondral lesions. Reviewing the two echoe separately has been shown to provide higher diagnostic sensitivity for cartilage lesions because of the higher T2 weighting of the second qDESS echo [14].

The T2 maps were primarily beneficial in assessing articular cartilage damage, particularly for subtle grade 1 and 2A lesions, and provided a higher sensitivity than conventional MRI with respect to arthroscopic findings. The lower specificity of the findings using qDESS plus T2 mapping may reflect the fact that T2 changes can precede morphologic changes by several years [13]. Some patients showed numerous foci of abnormal T2 values in areas of morphologically normal-appearing cartilage on conventional MRI and qDESS, which suggests that T2 maps may depict early chondral degeneration. Although T2 maps have also previously shown diagnostic promise for knee MRI, inefficient acquisition methods have rendered this technique clinically impractical [26]. A previous study showed promising utility of synthetic MRI in computing T2 relaxation time maps; however, the 2D sequence requiring 6.5 minutes of scan time had a voxel resolution of 0.92 mm^3 compared with a fivefold-higher resolution of 0.19 mm^3 using 5-minute 3D qDESS [29].

Discrepancies between conventional MRI and qDESS in the detection of abnormalities in the cruciate and collateral ligaments occurred primarily in the diagnosis of low- and moderate-grade sprains. Similarly, discrepancies occurred in the detection of myxoid degeneration (focal increased signal within the menisci without extension of signal abnormality to an articular surface). These abnormalities do not require surgical intervention and typically do not change the standard of care. Use of qDESS consistently decreased the depiction of bone marrow edema–like signal; however, the addition of a 2-minute coronal PD-weighted FS sequence significantly improved the detection of bone marrow edema and was beneficial in evaluating the collateral ligaments, which had lower diagnostic image quality scores. The additional PD-weighted FS sequence with image contrast that was more familiar to the readers also helped increase confidence in confirming cartilage, meniscus, and ligament findings. Low concordance in depicting tendinopathy was also observed with qDESS; however, even conventional MRI has low accuracy for detecting tendinopathy [30].

Similar to the T2 map generation, the deep learning–based super-resolution enhancement was a postprocessing method that did not affect the MRI acquisition time. Deep learning–based super resolution was previously found to be robust to artifact generation because it generates an image showing only a sparse difference between the low-resolution and high-resolution data [21]. This algorithm has been validated for maintaining T2 accuracy and image quality in evaluating chondral degeneration and osteophytes [22, 31]. The super-resolution technique mitigates the drawbacks of decreased image signal-to-noise ratio and biased T2 measurements that occur with higher-resolution MRI.

This study has several limitations. The readers could not be blinded to the sequences being used because of the inherent contrast in images. Additionally, this study retrospectively correlated changes in cartilage T2 values with arthroscopic findings. Future studies could prospectively review these T2 maps at the time of arthroscopic surgery, allowing more focused evaluation of articular cartilage. In the future, these early chondral signal alterations

in the T2 maps may be useful for guiding patient treatment and the need for subsequent follow-up. Although qDESS and the PD-weighted FS sequences provide fat-suppressed contrast, use of a Dixon PD sequence instead of the PD-weighted FS sequence could also generate simultaneous water-only and fat-only images. Moreover, additional multicenter studies showing consistency across different sites and scanners will be required before implementation of widespread clinical use.

In conclusion, we found that qDESS prospectively enhanced with deep learning–based super-resolution enabled rapid, high-resolution, multicontrast, and quantitative knee MRI. Imaging findings from qDESS were comparable to those from conventional knee MRI and had diagnostic accuracy nearly equivalent to conventional knee MRI with respect to arthroscopy. The ability of qDESS to automatically generate T2 maps without additional scan time may add value for clinical detection of cartilage abnormalities. The proposed 5-minute qDESS method has potential for future use in abbreviated knee MRI protocols.

Supplementary Material

Refer to Web version on PubMed Central for supplementary material.

Acknowledgments

Supported by grants R01 AR063643, R01 EB002524, K24 AR062068, and P41 EB015891 from the NIH; the Precision Health and Integrated Diagnostics Seed Grant from Stanford University; GE Healthcare (research support to G. E. Gold, B. A. Hargreaves, and K. J. Stevens); and Philips Healthcare (research support to B. A. Hargreaves). Neither GE Healthcare nor Philips Healthcare was involved in the design, execution, or analysis of this study.

References

1. van Beek EJR, Kuhl C, Anzai Y, et al. Value of MRI in medicine: more than just another test? J Magn Reson Imaging 2019; 49:e14–e25 [PubMed: 30145852]
2. Chaudhari AS, Kogan F, Pedoia V, Majumdar S, Gold GE, Hargreaves BA. Rapid knee MRI acquisition and analysis techniques for imaging osteoarthritis. J Magn Reson Imaging 2020; 52:1321–1339 [PubMed: 31755191]
3. Fritz J, Fritz B, Thawait GG, Meyer H, Gilson WD, Raithel E. Three-dimensional CAIPIRINHA SPACE TSE for 5-minute high-resolution MRI of the knee. Invest Radiol 2016; 51:609–617 [PubMed: 27187045]
4. Kijowski R, Davis KW, Woods MA, et al. Knee joint: comprehensive assessment with 3D isotropic resolution fast spin-echo MR imaging: diagnostic performance compared with that of conventional MR imaging at 3.0 T. Radiology 2009; 252:486–495 [PubMed: 19703886]
5. Del Grande F, Delcogliano M, Guglielmi R, et al. Fully automated 10-minute 3D CAIPIRINHA SPACE TSE MRI of the knee in adults: a multicenter, multi-reader, multifield-strength validation study. Invest Radiol 2018; 53:689–697 [PubMed: 30085948]
6. Bao S, Tamir JI, Young JL, et al. Fast comprehensive single-sequence four-dimensional pediatric knee MRI with T_2 shuffling. J Magn Reson Imaging 2017; 45:1700–1711 [PubMed: 27726251]
7. Welsch GH, Scheffler K, Mamisch TC, et al. Rapid estimation of cartilage T2 based on double echo at steady state (DESS) with 3 Tesla. Magn Reson Med 2009; 62:544–549 [PubMed: 19526515]
8. Chaudhari AS, Black MS, Eijgenraam S, et al. Five-minute knee MRI for simultaneous morphometry and T_2 relaxometry of cartilage and meniscus and for semiquantitative radiological assessment using double-echo in steady-state at 3T. J Magn Reson Imaging 2018; 47:1328–1341 [PubMed: 29090500]

9. Matzat SJ, McWalter EJ, Kogan F, Chen W, Gold GE. T2 relaxation time quantitation differs between pulse sequences in articular cartilage. J Magn Reson Imaging 2015; 42:105–113 [PubMed: 25244647]
10. Sveinsson B, Chaudhari AS, Gold GE, Hargreaves BA. A simple analytic method for estimating T2 in the knee from DESS. Magn Reson Imaging 2017; 38:63–70 [PubMed: 28017730]
11. Baum T, Joseph GB, Karampinos DC, Jungmann PM, Link TM, Bauer JS. Cartilage and meniscal T2 relaxation time as non-invasive biomarker for knee osteoarthritis and cartilage repair procedures. Osteoarthritis Cartilage 2013; 21:1474–1484 [PubMed: 23896316]
12. Eijgenraam SM, Chaudhari AS, Reijman M, et al. Time-saving opportunities in knee osteoarthritis: T_2 mapping and structural imaging of the knee using a single 5-min MRI scan. Eur Radiol 2020; 30:2231–2240 [PubMed: 31844957]
13. Kretzschmar M, Nevitt MC, Schwaiger BJ, Joseph GB, McCulloch CE, Link TM. Spatial distribution and temporal progression of T2 relaxation time values in knee cartilage prior to the onset of cartilage lesions: data from the Osteoarthritis Initiative (OAI). Osteoarthritis Cartilage 2019; 27:737–745 [PubMed: 30802496]
14. Chaudhari AS, Stevens KJ, Sveinsson B, et al. Combined 5-minute double-echo in steady-state with separated echoes and 2-minute proton-density-weighted 2D FSE sequence for comprehensive whole-joint knee MRI assessment. J Magn Reson Imaging 2019; 49:e183–e194 [PubMed: 30582251]
15. Blaimer M, Breuer F, Mueller M, Heidemann RM, Griswold MA, Jakob PM. SMASH, SENSE, PILS, GRAPPA: how to choose the optimal method. Top Magn Reson Imaging 2004; 15:223–236 [PubMed: 15548953]
16. Barth M, Breuer F, Koopmans PJ, Norris DG, Poser BA. Simultaneous multislice (SMS) imaging techniques. Magn Reson Med 2016; 75:63–81 [PubMed: 26308571]
17. Chen H, Zhang Y, Kalra MK, et al. Low-dose CT with a residual encoder-decoder convolutional neural network. IEEE Trans Med Imaging 2017; 36:2524–2535 [PubMed: 28622671]
18. Gong E, Pauly JM, Wintermark M, Zaharchuk G. Deep learning enables reduced gadolinium dose for contrast-enhanced brain MRI. J Magn Reson Imaging 2018; 48:330–340 [PubMed: 29437269]
19. Chen KT, Gong E, de Carvalho Macruz FB, et al. Ultra-low-dose ^{18}F-florbetaben amyloid PET imaging using deep learning with multi-contrast MRI in-puts. Radiology 2019; 290:649–656 [PubMed: 30526350]
20. Plenge E, Poot DHJJ, Bernsen M, et al. Super-resolution methods in MRI: can they improve the trade-off between resolution, signal-to-noise ratio, and acquisition time? Magn Reson Med 2012; 68:1983–1993 [PubMed: 22298247]
21. Chaudhari AS, Fang Z, Kogan F, et al. Super-resolution musculoskeletal MRI using deep learning. Magn Reson Med 2018; 80:2139–2154 [PubMed: 29582464]
22. Chaudhari AS, Stevens KJ, Wood JP, et al. Utility of deep learning super-resolution in the context of osteoarthritis MRI biomarkers. J Magn Reson Imaging 2020; 51:768–779 [PubMed: 31313397]
23. Noyes FR, Stabler CL. A system for grading articular cartilage lesions at arthroscopy. Am J Sports Med 1989; 17:505–513 [PubMed: 2675649]
24. Fritz J, Ahlawat S, Fritz B, et al. 10-Min 3D turbo spin echo MRI of the knee in children: arthroscopy-validated accuracy for the diagnosis of internal derangement. J Magn Reson Imaging 2019; 49:e139–e151 [PubMed: 30142235]
25. Smiley P, Wasilewski SA. Arthroscopic synovectomy. Arthroscopy 1990; 6:18–23 [PubMed: 2310444]
26. Kijowski R, Blankenbaker DG, Munoz Del Rio A, Baer GS, Graf BK. Evaluation of the articular cartilage of the knee joint: value of adding a T2 mapping sequence to a routine MR imaging protocol. Radiology 2013; 267:503–513 [PubMed: 23297335]
27. Landis JR, Koch GG. The measurement of observer agreement for categorical data. Biometrics 1977; 33:159–174 [PubMed: 843571]
28. Chaudhari AS, Sandino CM, Cole EK, et al. Prospective deployment of deep learning in MRI: a framework for important considerations, challenges, and recommendations for best practices. J Magn Reson Imaging 2020 Aug 24 [published online]

29. Roux M, Hilbert T, Hussami M, Becce F, Kober T, Omoumi P. MRI T2 mapping of the knee providing synthetic morphologic images: comparison to conventional turbo spin-echo MRI. Radiology 2019; 293:620–630 [PubMed: 31573393]

30. Warden SJ, Kiss ZS, Malara FA, Ooi ABT, Cook JL, Crossley KM. Comparative accuracy of magnetic resonance imaging and ultrasonography in confirming clinically diagnosed patellar tendinopathy. Am J Sports Med 2007; 35:427–436 [PubMed: 17261569]

31. Chaudhari A, Fang Z, Lee JH, Gold G, Hargreaves B. Deep learning super-resolution enables rapid simultaneous morphological and quantitative magnetic resonance imaging. In: Knoll F, Maier A, Rueckert D, eds. International Workshop on Machine Learning for Medical Image Reconstruction. Springer Nature, 2018: 3–11

HIGHLIGHTS

Key Finding

- A 5-minute quantitative double-echo steady-state (qDESS) sequence prospectively augmented with deep learning showed high agreement with conventional knee MRI findings and accuracy comparable with conventional knee MRI with respect to surgical findings. Automatic qDESS T2 relaxation time maps improve sensitivity for subtle cartilage lesions compared with conventional knee MRI.

Importance

- The 5-minute qDESS sequence may facilitate an abbreviated knee MRI protocol that provides additional quantitative information that is particularly helpful for detecting early cartilage degeneration.

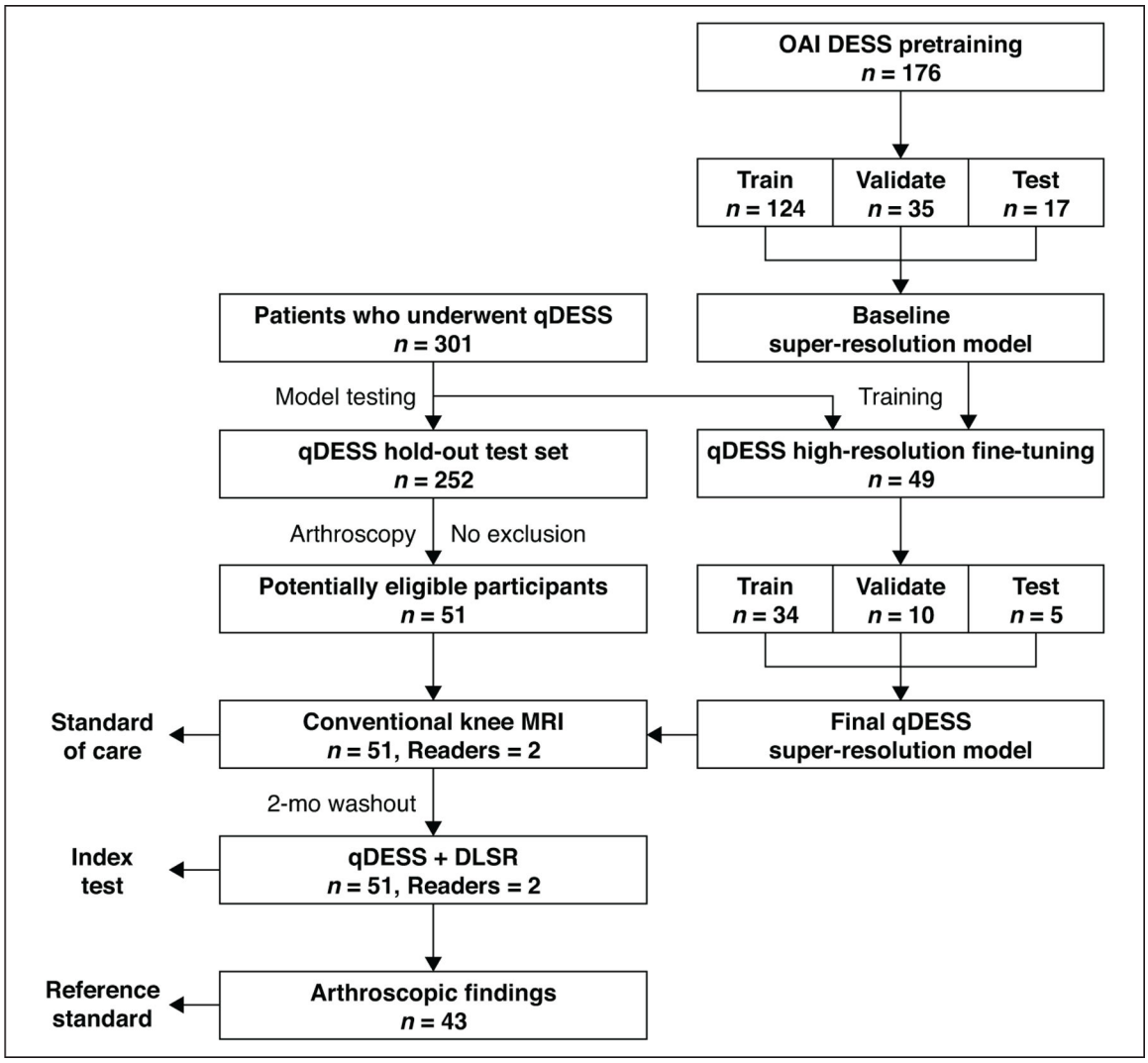

Fig. 1—.

Flowchart shows patient inclusion (*left*) and paradigm for training deep learning super-resolution (DLSR) algorithm (*right*). Super-resolution method was initially pretrained using 176 double-echo steady-state (DESS) scans with combined echoes from Osteoarthritis Initiative (OAI) [21]. Patients (n = 301) underwent quantitative DESS (qDESS). Imaging from 49 of these patients was used for subsequent fine-tuning of pretrained super-resolution method, and remaining 252 patients were eligible for study inclusion. Of those 252 patients, 51 underwent surgery and were included in final sample. Conventional MR and Qdess images from these patients were evaluated by two radiologists, with 2-month washout period between interpretations. Of 51 patients, 43 had arthroscopic reports with complete information for evaluating cartilage, menisci, ligaments, and synovium.

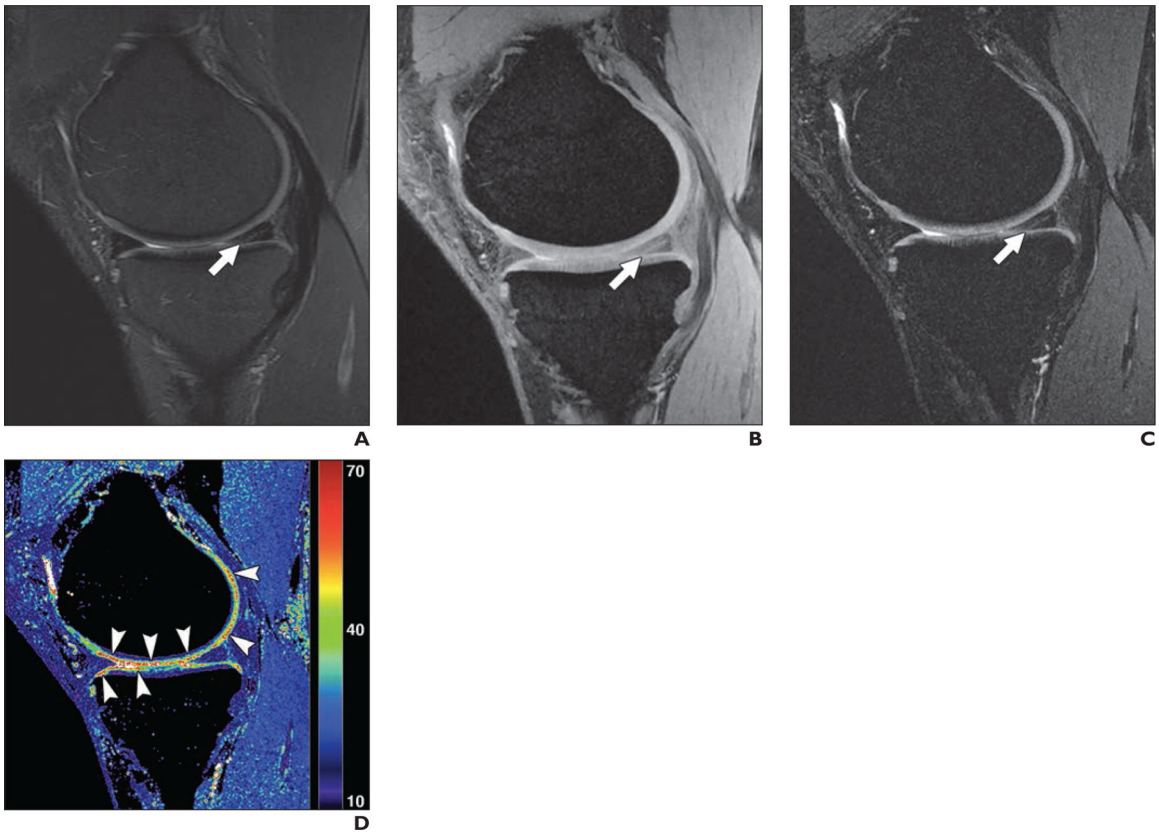

Fig. 2—.

41-year-old man with oblique tear in posterior horn of medial meniscus.

A, Sagittal T2-weighted MR image shows abnormal linear signal extending to inferior articular surface (*arrow*), indicating meniscal tear.

B and **C,** Quantitative double-echo steady-state (qDESS) MR images with S+ echo (**B**) and S–echo (**C**) also depict meniscal tear (*arrow*), similar to **A**.

D, qDESS T2 map (values in milliseconds) shows multiple foci (*arrowheads*) with abnormal T2 values in articular cartilage graded as normal by both readers in **A**–**C**. These focal increases in T2 were consistent with arthroscopic findings of extensive chondral softening along medial femoral condyle (grade 2B) and medial tibial plateau (grade 2A).

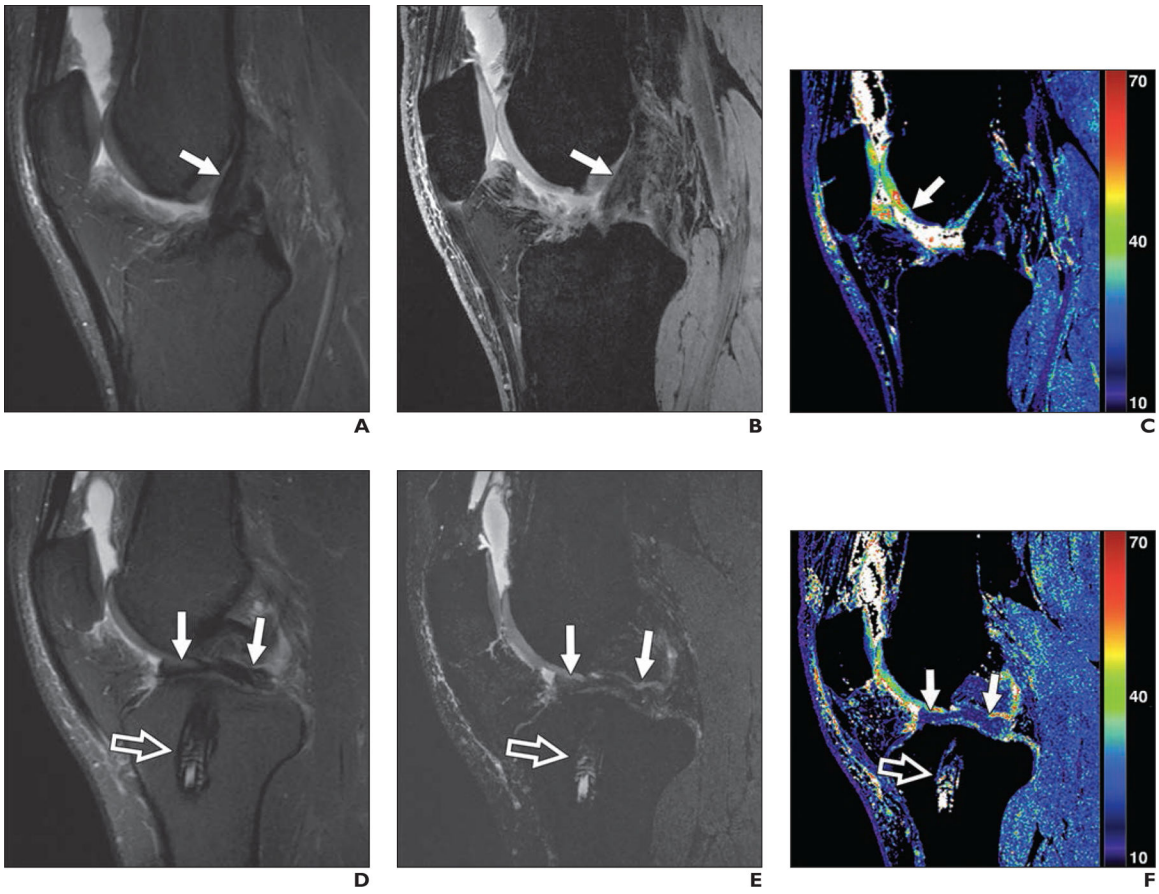

Fig. 3—.

30-year-old man with previous anterior cruciate ligament (ACL) reconstruction who experienced knee reinjury.

A, Sagittal T2-weighted MR image shows intact ACL graft with conspicuity (*arrow*).

B, Quantitative double-echo steady-state (qDESS) MR image with mixed T2- and T1-weighted echo shows conspicuity of ACL graft (*arrow*) similar to **A**.

C, qDESS T2 map (values in milliseconds) shows focal abnormal T2 relaxation (*arrow*) despite cartilage in trochlea graded as normal in **A** and **B**.

D, Sagittal T2-weighted MR image shows biointerference screw in tibial tunnel (*open arrow*) and arthroscopically proven bucket-handle tear of medial meniscus (*solid arrows*) with fragment displaced in intercondylar notch.

E and **F,** qDESS image with higher T2-weighted echo (**E**) and qDESS T2 map (**F**) show biointerference screw (*open arrow*) and meniscal tear (*solid arrows*) similar to **D**.

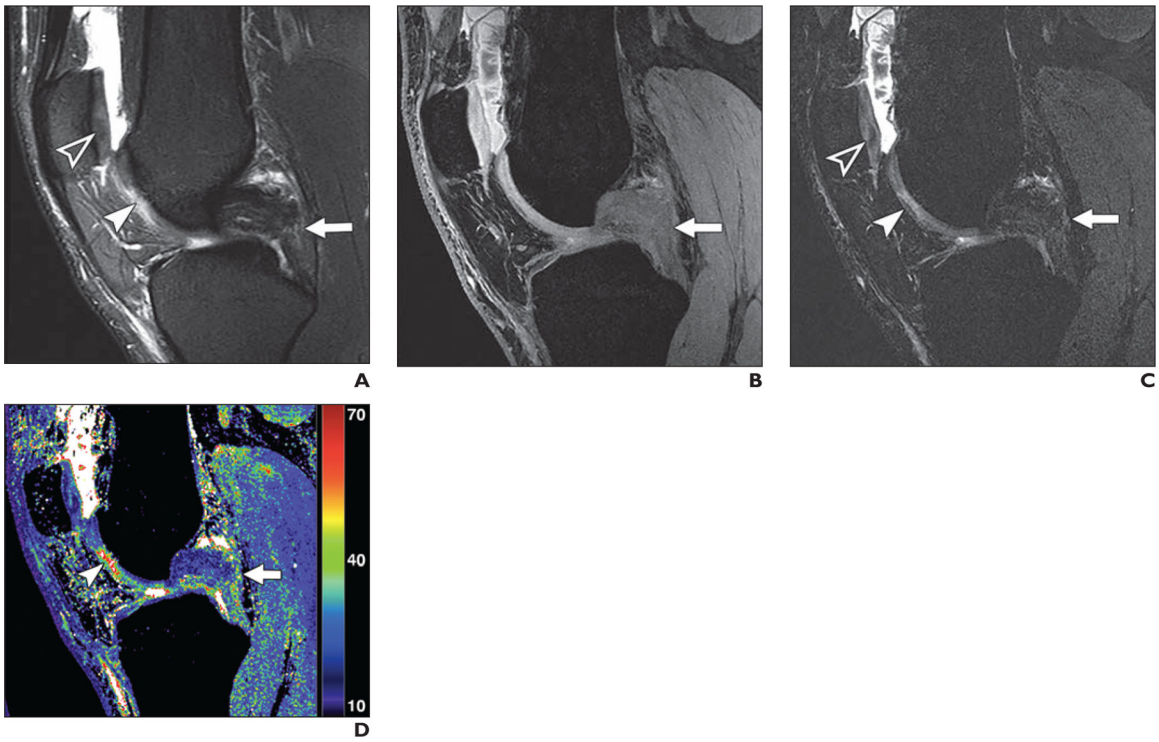

Fig. 4—.

19-year-old woman with high-grade tear of mid fibers in posterior cruciate ligament (PCL). **A,** Sagittal T2-weighted MR image shows PCL tear (*arrow*), focal chondral thinning (*solid arrowhead*), irregularity, and signal heterogeneity (*open arrowhead*) within central trochlea. **B,** Quantitative double-echo steady-state (qDESS) image with mixed T2-and T1-weighted echo also shows PCL tear (*arrow*). **C,** qDESS image with higher T2-weighted echo shows PCL tear (*arrow*), focal chondral thinning (*solid arrowhead*), and signal heterogeneity (*open arrowhead*) within central trochlea. **D,** qDESS T2 map (values in milliseconds) shows PCL tear (*arrow*) and striking T2 prolongation (*arrowhead*) within trochlear cartilage.

TABLE 1:

Scan Parameters for Conventional Knee MRI and the qDESS Protocol

Sequence	2D					3D Sagittal qDESS
	Axial Proton Density Fat-Saturated	Coronal T1-Weighted	Sagittal T2-Weighted Fat-Saturated	Sagittal Proton Density	Coronal Proton Density Fat-Saturated	
TR/TE	4000/35	600/18	5441/54	4000/35	4000/35	18.6/5.9
Flip angle (°)	142	142	142	142	142	20
Echo-train length	9	3	11	9	9	1
No. of signals acquired	3	3	4	2	2	1
Bandwidth (± kHz)	50	50	50	50	50	41.7
FOV (mm)	140 × 140	140 × 140	140 × 140	140 × 140	140 × 140	160 × 160
Acquisition matrix	512 × 224	416 × 224	384 × 192	384 × 224	384 × 224	416 × 512
Resolution (mm^2)	0.27 × 0.63	0.34 × 0.63	0.36 × 0.72	0.36 × 0.63	0.36 × 0.63	0.34 × 0.27
Slice thickness (mm)	3	2.5	2.5	2.5	2.5	1.6
Slice gap (mm)	0.3	0	0	0	0	0
No. of slices	36	44	40	40	44	80
Parallel imaging	2 × 1	NA	2 × 1	NA	2 × 1	2 × 1
Scan time (min:s)	2:56	2:18	3:43	3:28	2:00	5:00

Note—qDESS = quantitative double-echo steady-state, NA = not applicable.

AJR Am J Roentgenol. Author manuscript; available in PMC 2022 February 22.

TABLE 2:

Summary of All Abnormalities Detected on Conventional Knee MRI and qDESS for Both Readers and Interreader Agreement

	Conventional MRI			qDESS			
Tissue, Finding	**Reader 1**	**Reader 2**	**Agreement (%)**	**Reader 1**	**Reader 2**	**Agreement (%)**	**Surgical Findings[a]**
Meniscus							
Normal	56	51	95	61	50	89	56
Myxoid degeneration	4	8	92	2	17	85	0
Tear	42	43	97	39	35	98	32
Cruciate ligaments							
Normal	81	80	95	86	84	96	75
Low-grade sprain	3	4	97	0	0	96	0
Moderate sprain	5	6	99	4	6	99	0
Complete tear	13	12	99	12	11	99	11
Collateral ligaments							
Normal	137	137	97	145	137	95	–
Low-grade sprain	11	10	98	5	12	95	–
Moderate sprain	3	4	99	2	4	96	–
Complete tear	2	2	100	1	0	99	–
Cartilage							
Grade 0	180	168	92	184	150	87	0
Grade 1	4	8	99	0	0	95	24
Grade 2A	69	63	88	51	58	87	45
Grade 2B	26	37	94	39	52	93	44
Grade 3	27	30	99	32	30	97	22
Extensor mechanism							
Normal	70	63	83	92	86	90	–
Tendinopathy	27	32	85	8	12	90	–
Partial tear	5	7	98	2	4	98	–
Complete tear	0	0	NA	0	0	NA	–
Bone marrow							
Normal	804	795	95	842	837	98	–

	Conventional MRI			qDESS			
Tissue, Finding	**Reader 1**	**Reader 2**	**Agreement (%)**	**Reader 1**	**Reader 2**	**Agreement (%)**	**Surgical Findings[a]**
Bone marrow edema	68	72	93	31	35	93	–
Subchondral cyst	34	40	95	39	38	99	–
Fracture	12	11	98	6	8	98	–
Synovium							
Normal	34	31	95	34	32	92	–
Effusion	35	35	95	34	36	92	–
Synovitis	33	36	95	34	34	92	17

Note—Values are the number of findings unless otherwise indicated. Dash (−) indicates finding was not evaluated. qDESS = quantitative double-echo steady-state, NA = not applicable.

[a]Surgical findings are presented for 43 of 51 patients with imaging results.

AJR Am J Roentgenol. Author manuscript; available in PMC 2022 February 22.

TABLE 3:

Comparison of Positive, Negative, and Total Agreement Between Conventional Knee MRI and Quantitative Double-Echo Steady-State Findings

Tissue	Agreement (%)			Cohen κ (95% CI)[a]
	Positive Findings	Negative Findings	Total	
Meniscus	87 (78–93)	92 (85–96)	89 (84–93)	0.73 (0.66–0.80)
Cruciate ligaments	74 (59–86)	99 (96–99)	94 (89–97)	0.85 (0.76–0.94)
Collateral ligaments	59 (41–76)	98 (96–99)	94 (91–96)	0.71 (0.58–0.84)
Cartilage	87 (82–91)	86 (82–90)	87 (84–89)	0.73 (0.68–0.77)
Extensor mechanism	24 (15–36)	93 (88–97)	69 (62–75)	0.64 (0.52–0.76)
Bone barrow	51 (45–58)	98 (98–99)	92 (90–93)	0.83 (0.79–0.87)
Synovium	94 (89–97)	89 (79–96)	93 (88–96)	0.85 (0.78–0.93)

Note—Values are the mean with 95% CI in parentheses unless otherwise indicated. Findings are pooled per tissue type.

[a]Interreader agreement.

TABLE 4:

Sensitivity and Specificity for Conventional MRI and qDESS Protocols Compared With the Arthroscopic Reference Standard

Tissue, Sequence	Sensitivity (%)	Specificity (%)	Accuracy (%)	*p* [a]
Meniscus				
Conventional MRI	93 (84–98)	79 (71–87)	84 (78–89)	NA
qDESS	90 (79–96)	80 (72–87)	84 (77–89)	> .99
Cruciate ligaments				
Conventional MRI	91 (71–99)	87 (81–92)	88 (82–92)	NA
qDESS	86 (65–97)	91 (86–95)	91 (85–95)	.23
Cartilage				
Conventional MRI	58 (52–64)	73 (67–79)	66 (62–70)	NA
qDESS	54 (47–60)	66 (60–72)	60 (56–64)	.47
qDESS plus T2 mapping	73 (67–79)	55 (49–61)	64 (60–68)	.003
Synovium				
Conventional MRI	65 (46–80)	27 (16–41)	42 (31–53)	NA
qDESS	65 (46–80)	23 (13–37)	40 (29–51)	.62

Note—Values in parentheses are the 95% CI. Results were calculated by pooling all abnormalities per tissue type. qDESS = quantitative double-echo steady-state, NA = not applicable.

[a]Values signify differences in the sensitivity and specificity confusion matrix between qDESS (with and without T2 maps for cartilage) and conventional MRI.

TABLE 5:

Sensitivity and Specificity for Grading Cartilage Lesions on Conventional MRI, qDESS, and qDESS Plus T2 Mapping Compared With the Arthroscopic Reference Standard

Cartilage Lesion Grade, Sequence	Sensitivity (%)	Specificity (%)	Accuracy (%)	*p* [a]
1				
Conventional MRI	33 (20–48)	56 (51–60)	53 (49–58)	NA
qDESS	23 (12–37)	53 (49–58)	51 (46–55)	.81
qDESS plus T2 mapping	46 (31–61)	39 (35–44)	40 (35–45)	.80
2A				
Conventional MRI	27 (18–37)	53 (48–58)	48 (44–53)	NA
qDESS	26 (17–36)	52 (47–56)	47 (43–52)	.02
qDESS plus T2 mapping	58 (47–68)	40 (35–45)	43 (39–48)	< .001
2B				
Conventional MRI	81 (71–88)	64 (60–69)	67 (63–71)	NA
qDESS	76 (65–85)	62 (57–67)	65 (60–69)	.22
qDESS plus T2 mapping	86 (77–93)	46 (41–51)	53 (48–57)	.003
3				
Conventional MRI	93 (81–99)	61 (57–66)	64 (60–68)	NA
qDESS	93 (81–99)	60 (56–65)	63 (59–67)	.45
qDESS plus T2 mapping	98 (88–99)	44 (40–49)	49 (44–53)	.63

Note—Values in parentheses are the 95% CI. qDESS = quantitative double-echo steady-state, NA = not applicable.

[a]Values signify differences in the sensitivity and specificity confusion matrix between qDESS (with and without T2 maps for cartilage) and conventional MRI.